

RFQCOEF, A PACKAGE FOR EXTRACTING THE HARMONIC COEFFICIENTS FOR THE POTENTIAL FUNCTION IN AN RF QUADRUPOLE CELL

N.J. Diserens*
 Atomic Energy of Canada Limited, Research Company
 Chalk River Nuclear Laboratories
 Chalk River, Ontario, Canada K0J 1J0

Summary

In studying the beam dynamics within an rf quadrupole accelerator it is required to compute the potentials and fields rapidly. If an analytic function is to be used, the harmonic coefficients of the expressions must be calculated for each cell. A computer package has been developed which employs a 3 dimensional differential finite element method with about 1500 nodes to model a single 180° cell. A conjugate gradient solver is used. The harmonic coefficients of the potential function are obtained by a least squares method using the potentials at those nodes lying within a cylindrical area just inside the poles. The total calculation time per cell is about 30 CPU seconds on a CDC Cyber 175. Results are compared with those previously obtained by means of the CHR3D image charge program.

Introduction

The radiofrequency quadrupole accelerator (RFQ)¹ is an exciting recent development in linear accelerator technology, enabling high intensity ion beams to be accelerated and bunched in the same device.

In studying the beam dynamics in an RFQ it is desirable to parameterize the potential function within each of several hundred 'cells'. There is fairly smooth variation of parameters from one cell to its neighbour, so in practice it is sufficient to compute them only at every tenth cell and then interpolate. Until recently the potential distribution within an RFQ cell has been parameterized with the aid of a computer program CHR3D² which uses an image charge integral method.

This paper reports the development of a program which employs a 3 dimensional differential finite element method³ to obtain the potential distribution and then uses a least squares fit to obtain the harmonic coefficients directly from the nodal potentials which lie on an irregular mesh. Surface field intensities on the vanes are also computed by the program. The following sections describe the program structure, the mesh generator and a comparison of results and CPU requirements with the previously used CHR3D method.

Program Structure

The program has been constructed on a modular basis, each of which exists as a separate program. The reasons for this are twofold:

- (a) Shortage of available core on the CYBER 175 has been easiest to overcome by separating the various parts of the program.
- (b) The mesh generation and solver modules were also required for a separate project to investigate space charge and image charge effects.

The three modules from which the package has been built are a) mesh generator, b) matrix assembler and c) potential solver, (with surface field evaluation and coefficient extraction). Figure 1 shows a flow diagram of the respective modules.

* Visiting Scientist from Rutherford Appleton Laboratory, Oxfordshire, England.

MESH GENERATOR

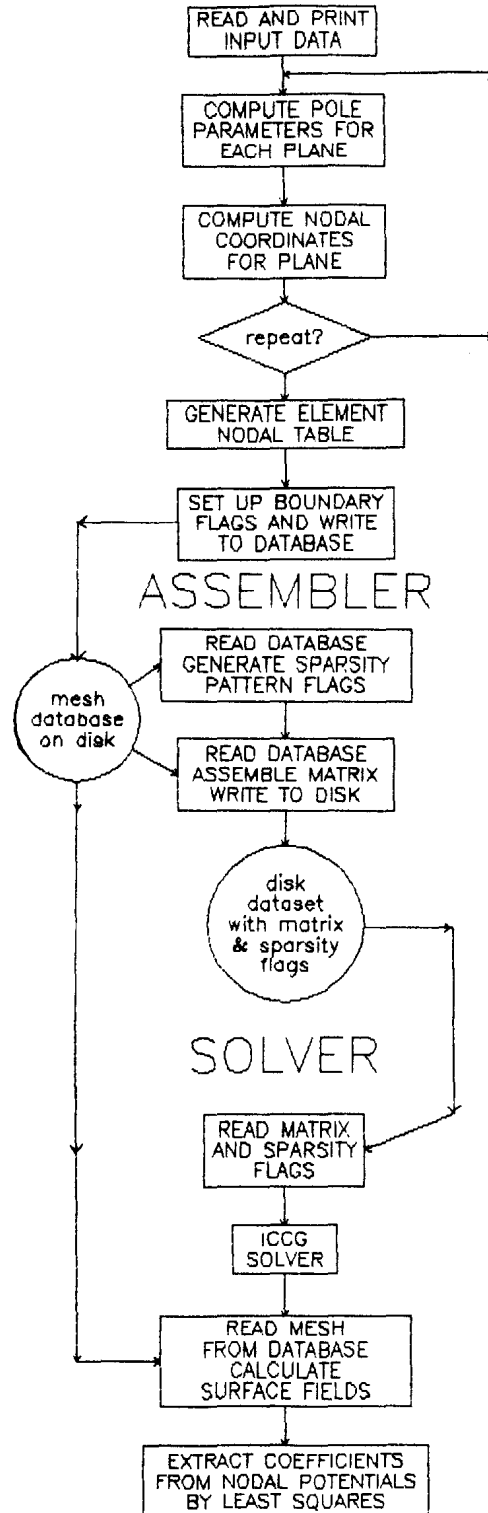


Fig. 1 Flow diagram.

Mesh Generator

Because of symmetry only one quadrant of the cell is modeled; the length is $\beta\lambda/2$. The mesh used is comprised entirely of 20 node isoparametric brick elements. All elements are of equal length in the axial (Z) direction. In the transverse (XY) planes the mesh topology is maintained throughout the length of the cell but because of the variation in the pole profile the dimensions of all elements change. However, the planes at the two ends of the cell are such that they are mirrors of each other, with X and Y directions interchanged.

The mesh generator subdivides the boundary such that there is the same number of mesh spacings, between the axis and each pole, as there is around each pole contour. The internal mesh is then constructed by interpolation. The element structure of a typical XY plane is shown in Fig. 2. Each plane is treated in this way and then the element nodal table is generated and the data is written to disk element by element.

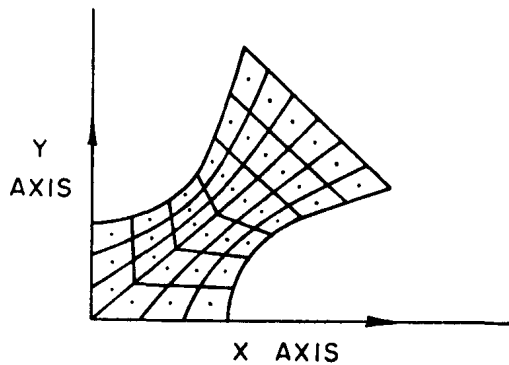


Fig. 2 A typical mesh cross section in an XY plane.

Matrix Assembly

The assembly and solver routines are designed to solve Poisson's Equation, $\epsilon \nabla^2 \phi + \rho = 0$, where ϕ is the potential, ρ is the charge density and ϵ the dielectric constant.

The matrix formulation for the finite element method gives:

$$\int ([B]^T [D] [B]) \{\phi\} + \{\rho\} [N] [N]^T dV = 0$$

where $[B]$ is the matrix of shape function derivatives, at the nodes, with respect to the X, Y and Z directions. $[D]$ is a matrix of material constants which here is a single term equal to the dielectric constant of free space. $\{\rho\}$ is a vector of nodal charge densities and $[N]$ is a matrix of element shape functions at the nodes. The expression $\int [B]^T [D] [B] dV$ is traditionally known as the 'stiffness matrix'.

For the problem to be solved here, the Laplace Equation, the charge densities are zero and the right hand sides of the equations to be solved are comprised of those terms pertaining to the known boundary potentials. The element data is first scanned in order to map the matrix sparsity pattern for the conjugate gradient solver. The sparsity pattern is a set of pointers showing the true positions of the non zero terms of the matrix which are stored in a compressed array. A second scan reads the nodal coordinates and uses the shape functions to construct the 'stiffness matrix' for each element, which is then added in to the main matrix array. The assembly is done with the whole matrix in core. The nodes on the end Z planes are

'slaved' together in a negative sense, use being made of the symmetry of the cell which has end planes that are mirror images of each other with the X and Y directions and also the potentials interchanged. At the end of this step the matrix is stored on disk.

Solver

The solver uses the Incomplete Cholesky Conjugate Gradient method (ICCG)⁴. This is a very efficient method which converges in about 11 iterations. About 50 iterations of the solver are required if the nodes of the end planes are not 'slaved' together.

The main advantage of the conjugate gradient method for this application is that it is an in-core solver. Also, the development work was ultimately directed towards representation of space charge, where the solver would need to be entered many times using the previous solution potentials as a starting point, and where the ICCG solver would be more efficient than most other methods.

Surface Fields

When the solution for the potentials has been obtained the element data is then scanned to determine which elements and which nodes lie on the pole surfaces. The electric fields at each surface node are calculated using the shape function derivatives and nodal potentials for each element. That is

$$E_x = - \frac{\partial \phi}{\partial x} = - \sum_{i=1}^{20} \frac{\partial N_i}{\partial x} \phi_i$$

and similarly for E_y and E_z .

Where two or more elements touch at a boundary there are slightly different values of fields calculated for the adjoining nodes for each of these elements. However, the variation is only about 0.5% and, as it is the maximum value which is sought, this will be the order of magnitude of the error.

A table of surface field components may be printed if required. The maximum value of the field is also output.

Extraction of Coefficients

The function used to describe the potential distribution in an rf quadrupole is:

$$\begin{aligned} U = & \{(C_{00}/a^2)r^2 \cos(2\theta) \\ & + C_{10} I_0(kr) \cos(kz) \\ & + (C_{01}/a^6)r^6 \cos(6\theta) \\ & + C_{11} I_4(kr) \cos(4\theta) \cos(kz) \\ & + C_{20} I_2(2kr) \cos(2\theta) \cos(2kz) \\ & + C_{21} I_6(2kr) \cos(6\theta) \cos(2kz) \\ & + C_{21} I_6(2kr) \cos(6\theta) \cos(2kz) \\ & + C_{30} I_0(3kr) \cos(3kz) \\ & + C_{31} I_4(3kr) \cos(4\theta) \cos(3kz) \end{aligned}$$

where the I_m values are the hyperbolic Bessel functions and k is π divided by the cell length. The coefficients are evaluated directly from the nodal potentials using a least squares fit. Only those potentials at nodes which lie within a radius smaller than the minimum pole radius are used. Weights are set at unity.

Table 1

Comparison of Coefficients obtained from CHR3D Package with those from RFQCOEF

Cell	a	M	CL	EFAC	C10	C00/a ²	C11	C01/a ⁶	C30	C20	C31	C21
20	0.409	1.020	0.58	1.301	0.00606	5.73007	0.05304	4.94852	0.0	-0.00003	0.0	0.00072
				1.294	0.00601	5.74846	0.05031	4.41814	0.0	-0.00002	-0.00001	-0.00077
60	0.399	1.072	0.60	1.339	0.02273	5.73981	0.20874	4.89934	0.0	0.00003	0.0	-0.00031
				1.335	0.02280	5.75573	0.21751	4.51230	0.0	-0.00006	-0.00001	0.00402
100	0.392	1.111	0.68	1.347	0.04307	5.74320	0.45675	4.88818	0.0	0.00018	0.0	0.00087
				1.345	0.04296	5.75630	0.48357	4.03974	-0.00001	0.00022	-0.00002	0.00628
140	0.381	1.171	0.92	1.324	0.09684	5.74616	1.40462	4.74544	0.0	0.00076	0.0	-0.04081
				1.324	0.09662	5.75831	1.35976	3.84250	0.0	0.00096	-0.00015	-0.09994
180	0.309	1.631	1.94	1.437	0.44918	5.65552	-36.14094	2.36514	-0.00002	-0.04355	-0.10643	-100.715
				1.384	0.44807	5.66045	-34.26460	1.44060	-0.00007	-0.04664	-0.10646	-99.0374

The upper value of each pair is the value from CHR3D, the lower is that from RFQCOEF.

Comparison with CHR3D Results

Prior to development of this package an image charge method known as CHR3D had been employed to extract the coefficients. The latter program computes the potentials over a cylinder within the minimum pole radius and uses a Fourier analysis to extract the harmonics. The running time of the CHR3D program on the Cyber 175 is about 30 minutes to extract one set of coefficients. With the RFQCOEF package it is found that sufficient accuracy is obtained using a mesh of 6 x 6 quadratic brick elements in each plane and 8 planes of elements in the axial direction. The total running time to extract one set of coefficients on the Cyber 175 is about 30 seconds.

Table 1 shows the values of the coefficients obtained by the two methods and also gives values of the enhancement factor, which is given by:

$$EFAC = \frac{\text{Maximum Surface Field}}{\text{Voltage between Vanes}} \times \frac{R_0}{Z}$$

where R_0 is the distance from the beam axis to the pole tips at the midplane of the cell.

The transverse radius of curvature of the pole tips was 0.348 cm for all cells. The vanes were tapered, from the radiused tips, to give a maximum width of 2.2 cm at 2.817 cm from the beam axis. A discrepancy in the enhancement factor values became noticeable as the cell length was increased. Also, a difference in the values of C_{01} became more marked, being about 60% at the highest number cell. Therefore, a further check was done against a program POTRFO⁵ which uses a series solution method. The cell dimensions used for this check were: a = 0.33 cm, M = 1.489. All other dimensions were the same as for the examples in Table 1. With a potential of 76 kV between the vanes the calculated pole tip fields were:

- (a) with RFQCOEF 14.50 and 23.81 MV/M
- (b) with POTRFO 14.58 and 23.64 MV/M.

This is regarded as confirmation that the surface field values given by RFQCOEF are reliable to better than 1% and would suggest that the CHR3D gives a value which is about 3% high for the longer cells. It also indicates that the coefficient values are likely to be more reliable than those from CHR3D. The large discrepancy in the C_{01} values at the high energy end of the RFO will have little effect on the beam dynamics.

The number of mesh elements used in these tests is near the practical limit available on the Cyber 175 using the ICCG in-core solver. Tests with varying numbers of mesh elements in each direction indicate that only the higher order coefficients show a significant change from one run to another.

Even with elements which are very elongated in the Z direction the discrepancy in potential values obtained throughout the beam region is well below 1% compared with those obtained when the mesh elements are of equal size in each direction. This means that so long as a complete set of coefficients is used from any one run the fit will be good.

Conclusions

A program which will enable RFO potential harmonic coefficients to be evaluated rapidly has been developed. This program could eventually be integrated into a larger package so that the coefficients were obtained for a whole RFO in one run. By this means the potential solution for each stage would be used as a starting point for the next, and the time spent in the solution routines would be reduced by about 60%.

References

1. I.M. Kapchinskii and V.A. Teplyakov, "Linear Ion Accelerator with Spatially Homogenous Strong Focusing", Prihory i. Teknika Eksperimenta 119, No. 2, pp. 19-22, March-April 1970.
2. K.R. Crandall, "Effects of Vane-Tip Geometry on the Electric Fields in Radio Frequency Quadrupole Linacs", Los Alamos National Laboratories, Report LA-9695-MS (1983).
3. O.C. Zienkiewicz, "The Finite Element Method", 3rd Ed., McGraw Hill, 1977.
4. D.A.H. Jacobs, "Preconditioned Conjugate Gradient Methods for Solving Large Systems of Algebraic Equations derived from Partial Differential Equations", CERL Note No. RD/L/N 55/80.
5. B.G. Chidley, G.E. McMichael and G.E. Lee-Whiting, "Design of RFO Vane Tip to Minimize Sparking Problems", IEEE Trans. Nucl. Sci., NS-30, 3560 (August 1983).